



## Evolution of $Ti_3Ni_4$ precipitates in $Ti_{49.2}Ni_{50.8}$ alloy during equal channel angular pressing

Jia-rui REN<sup>1</sup>, Alexander V. SHUITCEV<sup>1</sup>, Bin SUN<sup>2</sup>, Feng CHEN<sup>1</sup>, Li LI<sup>1</sup>, Yun-xiang TONG<sup>1</sup>

1. Institute of Materials Processing and Intelligent Manufacturing,  
College of Materials Science and Chemical Engineering, Harbin Engineering University, Harbin 150001, China;

2. Center of Testing and Analysis, College of Materials Science and Chemical Engineering,  
Harbin Engineering University, Harbin 150001, China

Received 8 May 2020; accepted 10 December 2020

**Abstract:** The evolution of  $Ti_3Ni_4$  precipitates in  $Ti_{49.2}Ni_{50.8}$  alloy during equal channel angular pressing (ECAP) and intermediate annealing was investigated by transmission electron microscopy. The solution-treated  $Ti_{49.2}Ni_{50.8}$  alloy was aged at 450 °C for 10 to 60 min to obtain  $Ti_3Ni_4$  precipitates ranging from 37 to 75 nm. After ECAP at 450 °C for one pass,  $Ti_3Ni_4$  precipitates introduced by aging for 10 and 30 min totally dissolve into the matrix; however, those produced by aging for 60 min become smaller. The critical size of  $Ti_3Ni_4$  precipitates to totally dissolve into matrix is determined to be in the range of 37–68 nm. The dislocation density of ECAP-processed samples depends on the initial size of  $Ti_3Ni_4$  precipitates after aging. With increasing the duration of initial aging from 10 to 60 min, the dislocation density firstly increases and then decreases.

**Key words:** TiNi shape memory alloy; equal channel angular pressing; dislocation; precipitation;  $Ti_3Ni_4$  phase

### 1 Introduction

TiNi-based shape memory alloys (SMAs) have drawn much attention in engineering and biomedical fields due to their superior functional properties and excellent biocompatibility [1–3]. The functional properties, such as shape memory effect and superelasticity can be controlled by tailoring microstructure. It is commonly accepted that grain refinement is effective in improving not only the functional properties but also the mechanical properties of TiNi-based SMAs [4–8]. Equal channel angular pressing (ECAP) has been often used in recent years to refine the microstructure of TiNi-based SMAs to ultrafine scale [9,10]. The grain size of TiNi-based SMAs can be reduced to be smaller than 300 nm [6–8,11–14].

During ECAP, in addition to the aforementioned grain refinement, other changes of microstructure take place, such as the dissolution of precipitates and the introduction of high density dislocations. For TiNi-based SMAs, ECAP is usually carried out at 400–500 °C and intermediate annealing is also required in order to eliminate severe work-hardening. Such a high processing temperature results in the precipitation of  $Ti_3Ni_4$  phase in Ni-rich TiNi SMAs. It has been reported that  $Ti_3Ni_4$  precipitates dissolve into the matrix due to severe plastic deformation [7,15,16]. SONG et al [17] found that after ECAP at 500 °C for one pass,  $Ti_3Ni_4$  precipitates in  $Ti_{49.3}Ni_{50.7}$  alloy initially aged at 500 °C for 20 min totally dissolve into the matrix. In contrast,  $Ti_3Ni_4$  precipitates in  $Ti_{49.1}Ni_{50.9}$  alloy initially aged in the same condition partially dissolve even after eight passes. ZHANG et al [12]

reported that for  $Ti_{49.1}Ni_{50.9}$  alloy processed by ECAP at 500 °C,  $Ti_3Ni_4$  precipitates do not dissolve into the matrix totally. The above inconsistency is suggested to be partially related to the dislocations introduced by ECAP, i.e., these dislocations influence the precipitation behavior during intermediate annealing.

$Ti_3Ni_4$  phase has an effect on the obtained microstructure and martensitic transformation for Ni-rich TiNi SMAs processed by ECAP. Our results show that  $Ti_3Ni_4$  phase favors refining the final microstructure of  $Ti_{49.2}Ni_{50.8}$  alloy processed by ECAP at 450 °C for eight passes [7]. In addition, the partial-dissolution of  $Ti_3Ni_4$  precipitates is responsible for the multiple-stage martensitic transformation in the ECAP-processed  $Ti_{49.2}Ni_{50.8}$  alloy [18].  $Ti_3Ni_4$  precipitates are effective in modifying the transformation behavior and improving shape recovery properties. Thus, it is of crucial importance to understand the dissolution behavior during ECAP and the precipitation behavior during intermediate annealing.

In the present work,  $Ti_{49.2}Ni_{50.8}$  (at.%) alloy was initially aged for different durations to obtain  $Ti_3Ni_4$  precipitates with various sizes and volume fractions. The aged alloys were processed by ECAP followed by intermediate annealing. The evolution of  $Ti_3Ni_4$  precipitates during ECAP and intermediate annealing was investigated. Special attention was paid to the role of dislocation. Based on the microstructural results, the related mechanism was discussed.

## 2 Experimental

Before ECAP, the commercially available  $Ti_{49.2}Ni_{50.8}$  alloy was firstly heat-treated. The heat treatments include solution treatment at 900 °C for 1 h and aging at 450 °C for 10, 30 and 60 min, respectively. The rod samples with a diameter of 10 mm and a length of 60 mm were processed by ECAP at 450 °C using a die with a channel-intersection angle of 120°. The samples were intermediately annealed at 450 °C for 10 min in a furnace before each pass and transferred to the pre-heated die as quickly as possible. The extrusion rate was fixed at 15 mm/s and the pressing route Bc was selected.  $Ti_3Ni_4$  precipitates and dislocations were examined with transmission electron microscopy (TEM, Talos F200X G2) operated at

200 kV. The bright-field imaging, high resolution imaging and selected area electron diffraction (SAED) techniques were used. The TEM foils were prepared by mechanical grinding, followed by twin-jet electropolishing. The electrolyte solution consisted of 95 vol.% acetic acid and 5 vol.% perchloric acid.

## 3 Results and discussion

### 3.1 $Ti_3Ni_4$ precipitates

Figure 1 shows the TEM bright field images and the corresponding SAED pattern of the aged  $Ti_{49.2}Ni_{50.8}$  alloy. After aging, the nanosized and coherent  $Ti_3Ni_4$  phase precipitates in the matrix. The size and volume fraction of precipitates in the samples subjected to various aging treatments are summarized in Table 1. The volume fraction was determined by Glagolev method [19]. Figure 2 shows the TEM bright field images of the samples after one ECAP pass. As compared to Fig. 1, the amount and size of  $Ti_3Ni_4$  precipitates are significantly reduced due to severe plastic deformation. For the samples initially aged for 10 and 30 min,  $Ti_3Ni_4$  precipitates are hardly observed except for those indicated by the arrows, as shown in Figs. 2(a) and (b). For the sample initially aged for 60 min,  $Ti_3Ni_4$  precipitates still exist, but their volume fraction is considerably reduced from  $(32.1\pm 3.3)\%$  to  $(14.2\pm 1.5)\%$  and the average size decreases from  $(74.7\pm 5.0)$  to  $(24.1\pm 2.6)$  nm, as shown in Fig. 2(c) and Table 1. Figure 2(d) shows the SAED pattern corresponding to Fig. 2(c). The pattern is characterized by the  $1/7[312]$  spots, which confirms the existence of  $Ti_3Ni_4$  phase. The above results indicate that  $Ti_3Ni_4$  precipitates can be dissolved by ECAP, being well consistent with the previous results [7,16–18].

In order to reveal the dissolution mechanism of  $Ti_3Ni_4$  phase, high resolution TEM observation was carried out for the sample that was initially aged for 10 min and processed by ECAP for one pass. The results are shown in Fig. 3. From Fig. 3(a), an irregular  $Ti_3Ni_4$  particle like a bow tie is observed, which is surrounded by dash line. The particle was identified by the diffraction pattern shown in the upper-right inset of Fig. 3(a) which is the result of Fourier transformation of Region A. The diffraction pattern on the bottom-left of Fig. 3(a) was taken from Region B. No diffraction spots of  $Ti_3Ni_4$  phase

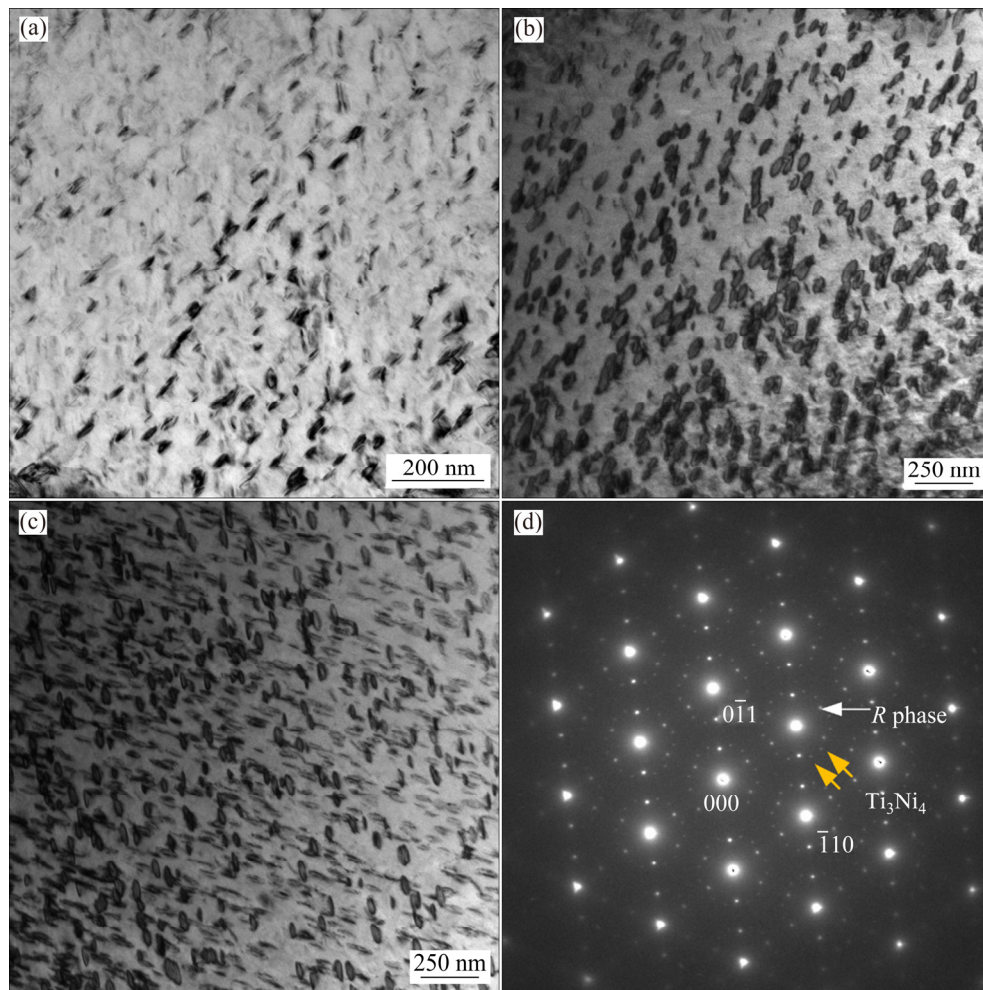


**Fig. 1** TEM bright field images of samples initially aged for 10 min (a), 30 min (b) and 60 min (c), and SAED pattern (d) taken from (c) (The diffraction spots of  $\text{Ti}_3\text{Ni}_4$  phase are indicated by the orange arrows)

**Table 1** Size and volume fraction of  $\text{Ti}_3\text{Ni}_4$  phase in samples after different treatments

Treatment	Size/nm			Volume fraction/%		
	10 min	30 min	60 min	10 min	30 min	60 min
0 p	37.2±4.4	68.2±4.61	74.7±5.0	12.9±1.8	24.3±3.8	32.1±3.3
1 p	—	—	24.1±2.6	—	—	14.2±1.5
1 p + intermediate annealing	21.8±3.2	49.7±4.9	22.4±2.9	9.2±1.6	13.0±1.5	31.3±3.2

p: ECAP pass

can be identified, implying that Region *B* is the matrix. Figure 3(b) is the result of inverse Fourier transformation of the rectangle region marked by the yellow line. The edge dislocation indicated by an arrow is observed in  $\text{Ti}_3\text{Ni}_4$  particle. The dislocation may be introduced through the following two ways: (1) shear deformation which makes the dislocation move into the dissolving  $\text{Ti}_3\text{Ni}_4$  precipitates, and (2) generation due to the conservation of Burgers vector [20]. The presence

of dislocation in  $\text{Ti}_3\text{Ni}_4$  particle implies that the dislocations should take part in the dissolution of precipitates. The spherical  $\text{Ti}_3\text{Ni}_4$  particle with a size of about 15 nm is also observed, as shown in the area circled by the dash line in Fig. 3(c), whose diffraction pattern is shown in the inset of Fig. 3(c).

It is suggested that  $\text{Ti}_3\text{Ni}_4$  precipitates change in the sequence of lens-shaped precipitates (aged sample) → fractured ones → spherical ones and dissolved ones. Based on the model proposed by

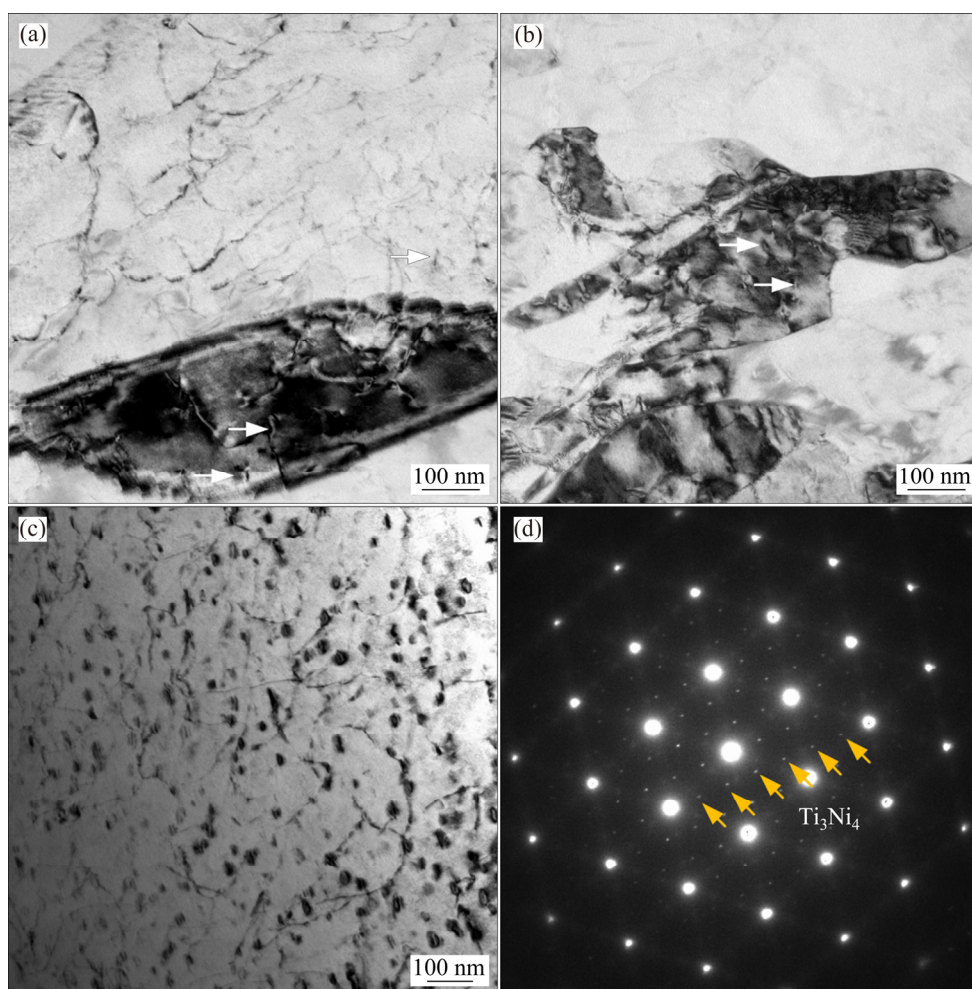


**Fig. 2** TEM bright field images of samples initially aged at 450 °C for 10 min (a), 30 min (b) and 60 min (c) after ECAP for one pass, and SAED pattern (d) taken from (c)

VASIĆEV et al [20], this evolution is schematically illustrated in Fig. 3(d), in which the dash line represents the slip plane, “solid symbol” represents the dislocations introduced by shear deformation and “blank symbol” represents those introduced due to the conservation of Burgers vector. Before ECAP, the initial  $Ti_3Ni_4$  particles are characterized by the regular lenticular shape. After ECAP for one pass,  $Ti_3Ni_4$  particles are broken to several parts by the dislocations passing through, leading to the formation of Cottrell atmosphere, which may take away the solute atom. This is suggested to be responsible for the dissolution of  $Ti_3Ni_4$  phase. The irregular and broken  $Ti_3Ni_4$  precipitates tend to achieve the state with minimum surface energy and gradually become spherical through the diffusion of solute atom. Once their size is less than a critical value,  $Ti_3Ni_4$  precipitates totally dissolve into the matrix.

The effect of initial aging treatment on the evolution of  $Ti_3Ni_4$  precipitates during ECAP is possibly related to the size and distribution of precipitates. It is well accepted that the critical stress of Frank–Read source for the dislocation multiplication is inversely proportional to the interparticle distance, and the shear stress of cutting the particles is directly proportional to the size and volume fraction of particles [21]. It is suggested that  $Ti_3Ni_4$  precipitates can be cut by the dislocation during ECAP due to their small size and coherency with matrix. This is supported by the results shown in Fig. 2 and the reported results in Ref. [16]. For the samples initially aged for 10 and 30 min, the distance between two neighboring particles is larger than that in the sample initially aged for 60 min, resulting in lower critical stress for dislocation multiplication. The shear stress of cutting the precipitates is also lower than that of the sample

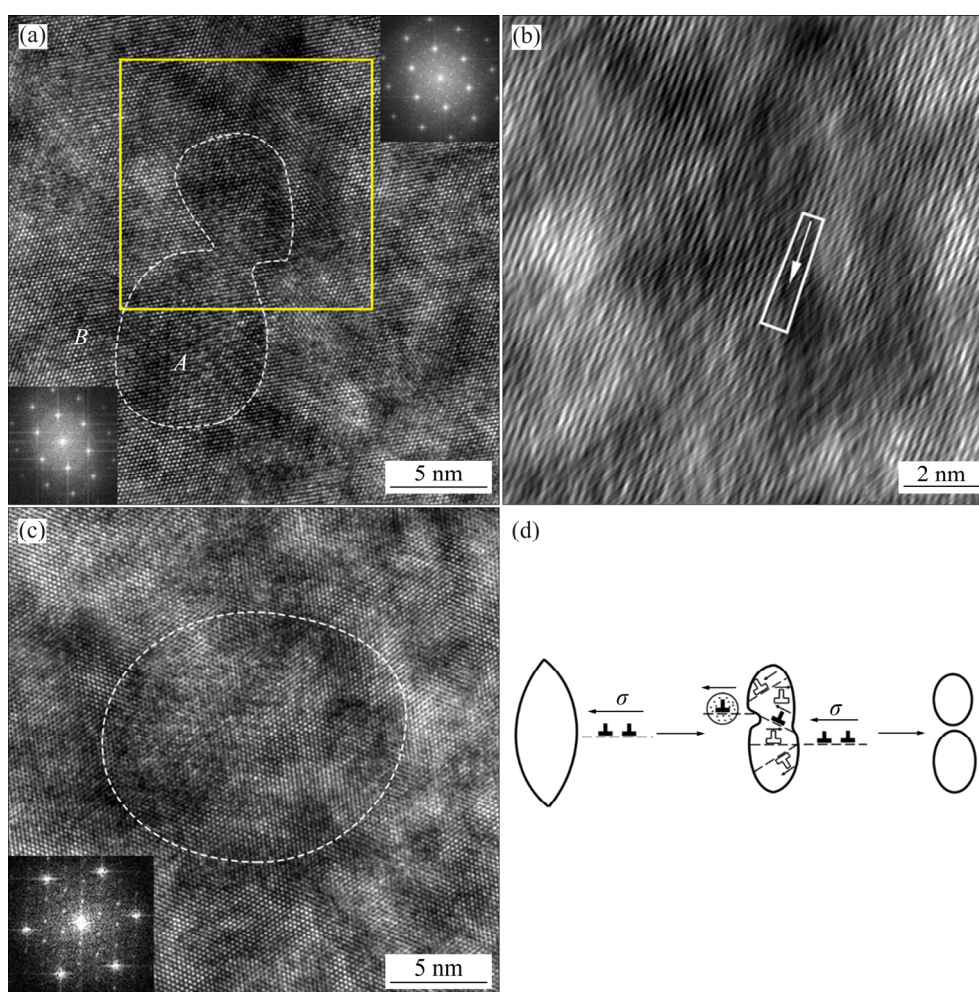


**Fig. 3** HRTEM image of sample initially aged at 450 °C for 10 min after ECAP for one pass (The upper-right and lower-left insets are the FFT diffraction patterns of Regions *A* and *B*, respectively) (a), IFT image (b) of rectangle region marked by yellow line in (a), HRTEM image of sample initially aged at 450 °C for 10 min after ECAP for one pass from another region (The lower-left inset is the FFT diffraction pattern of the circular region) (c), and schematic illustration of evolution of  $\text{Ti}_3\text{Ni}_4$  precipitates during ECAP for one pass (d)

aged for 60 min. Therefore,  $\text{Ti}_3\text{Ni}_4$  precipitates can be easily broken and dissolved because of the dislocation multiplication in these two samples. If the initial aging duration is increased to 60 min, the size of  $\text{Ti}_3\text{Ni}_4$  precipitates increases and the distance between two neighboring particles decreases. This leads to the increase of critical stress for dislocation multiplication and shear stress of cutting the particles. Therefore,  $\text{Ti}_3\text{Ni}_4$  precipitates partially dissolve into the matrix after ECAP.

### 3.2 Dislocation

The dislocation density of the samples processed by ECAP was measured by TEM. Figure 4 shows the typical dislocation morphology observed in different samples processed for one

pass. Several diffraction vectors  $\mathbf{g}$  were used to reduce the effect of extinction, including  $[\bar{1}10]_{B_2}$ ,  $[\bar{1}01]_{B_2}$  and  $[0\bar{1}1]_{B_2}$ . For simplicity, only the TEM images obtained under the vector of  $[\bar{1}10]_{B_2}$  are shown. The dislocation density was determined to be  $1.37 \times 10^{10}$ ,  $1.76 \times 10^{10}$ , and  $1.15 \times 10^{10} \text{ cm}^{-2}$ , for the samples initially aged for 10, 30, and 60 min, respectively.

The dislocations introduced by ECAP not only influence the dissolution of  $\text{Ti}_3\text{Ni}_4$  phase as mentioned above, but also affect the precipitation behavior of  $\text{Ti}_3\text{Ni}_4$  phase during the intermediate annealing. In order to reveal the above effect, the samples processed for one pass were annealed at 450 °C for 10 min. Their TEM images are shown in Fig. 5, from which the size and volume fraction of

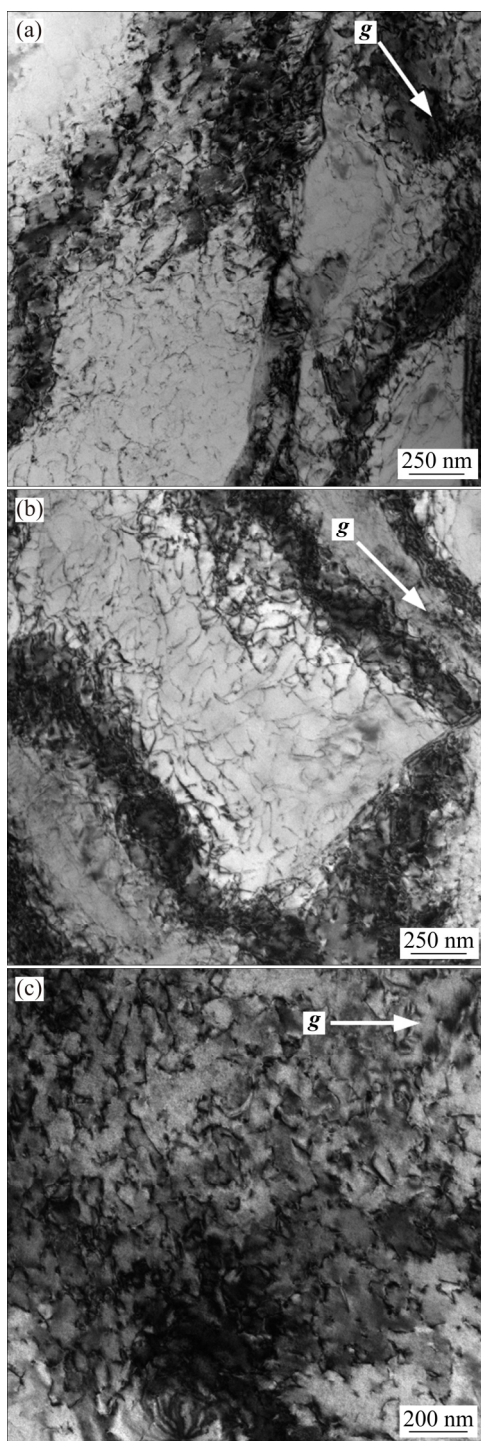


**Fig. 4** Typical dislocation morphologies in samples initially aged at 450 °C for 10 min (a), 30 min (b) and 60 min (c) after ECAP for one pass (The operational vector is  $[\bar{1}10]_{B2}$ )

$Ti_3Ni_4$  precipitates were calculated and listed in Table 1. After intermediate annealing,  $Ti_3Ni_4$  phase precipitates again in the samples initially aged for 10 and 30 min, respectively. The size of precipitates is directly proportional to the dislocation density.

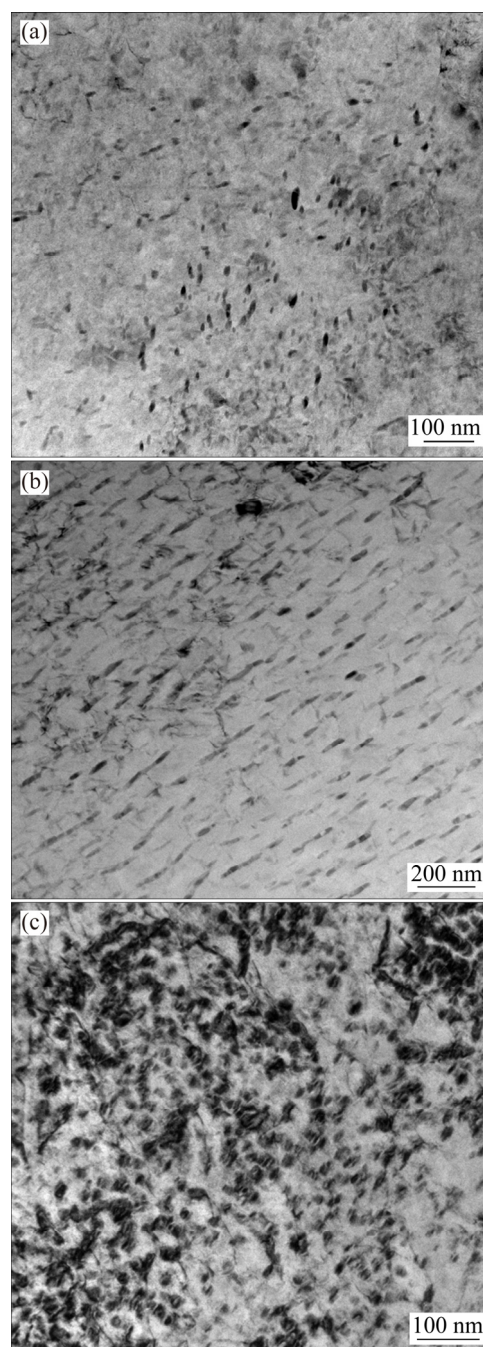


**Fig. 5** TEM bright field images of samples initially aged at 450 °C for 10 min (a), 30 min (b) and 60 min (c) after ECAP for one pass and annealing at 450 °C for 10 min

This is reasonable since the dislocation may accelerate the atom diffusion through acting as the diffusion channel. As compared to the  $Ti_3Ni_4$  precipitates formed during initial aging for 10 min, the  $Ti_3Ni_4$  precipitates in the ECAP-processed sample are characterized by the smaller size and volume fraction. This is possibly related to the constraint from internal stress-field, which is

supported by the previously reported results in which the precipitation of  $Ti_3Ni_4$  phase was suppressed by grain refinement [13]. For the sample initially aged for 30 min, it is surprising to note that  $Ti_3Ni_4$  precipitates grew up to  $(49.7\pm 4.9)$  nm. For the sample initially aged for 60 min, the size of precipitates decreases slightly, but the volume fraction increases as compared to those in the sample processed for one pass. Combined with the results shown in Fig. 2, it is suggested that the microstructural evolution of this sample is governed by the growth of residual precipitates and the nucleation and growth of newly formed  $Ti_3Ni_4$  precipitates. The newly formed  $Ti_3Ni_4$  precipitates may have smaller size.

Based on the results shown in Table 1, it is concluded that for the true strain of 0.6 imposed by the present ECAP for one pass, the critical size of  $Ti_3Ni_4$  precipitates to totally dissolve into the matrix is estimated to be in the range between 37 and 68 nm. Therefore, it is naturally reasonable to suggest that the aforementioned inconsistency reported in the previous works [7,12,17] is related to the initial microstructure resulting from the composition and the aging treatment. In those works,  $Ti_{49.1}Ni_{50.9}$  alloy [12] and  $Ti_{49.2}Ni_{50.8}$  alloy [7] were aged at 500 °C for 20 min or 450 °C for 15 min before each ECAP pass, respectively. This indicates that  $Ti_3Ni_4$  precipitates in the former are larger than the critical size to totally dissolve as compared to that in the latter because of excessive Ni, higher aging temperature and longer aging duration.

It is envisaged that the evolution of  $Ti_3Ni_4$  precipitates may influence the functional properties of as-ECAP processed TiNi alloys in the following ways: (1) causing the inhomogeneous distribution of Ni, (2) increasing the Ni content of matrix and (3) strengthening the matrix through Cottrell atmosphere [21]. The first way may be responsible for the multiple-stage transformation observed in as-ECAP processed Ni-rich TiNi alloys [8]. The latter two ways reduce the transformation temperatures because of the high sensitivity of transformation on Ni content and the enhanced resistance to transformation. This implies that the dissolution of  $Ti_3Ni_4$  phase influences martensitic transformation of ECAP-processed Ni-rich TiNi alloys besides the grain refinement and the introduced dislocation. Further investigation is

carrying out to comprehensively understand the detailed contributions from these different influencing mechanisms.

## 4 Conclusions

(1) During ECAP, the evolution of  $Ti_3Ni_4$  precipitates can be influenced by the initial aging treatment. When  $Ti_{49.2}Ni_{50.8}$  alloy is initially aged at 450 °C for less than 30 min,  $Ti_3Ni_4$  precipitates totally dissolve into the matrix after ECAP for one pass. When  $Ti_{49.2}Ni_{50.8}$  alloy is initially aged at 450 °C for 60 min, the size of  $Ti_3Ni_4$  precipitates reduces.

(2) For the first pass of ECAP having an imposed strain of 0.6, the critical size of  $Ti_3Ni_4$  precipitates to totally dissolve into the matrix is in the range between 37 and 68 nm.

(3) After the intermediate annealing at 450 °C for 10 min,  $Ti_3Ni_4$  precipitates form in the matrix again. The size of precipitates is inversely proportional to the dislocation density introduced during the last ECAP.

## Acknowledgments

The authors are grateful for the financial supports from the National Natural Science Foundation of China (51671064), and the National Key R&D Program of China (2017YFE0123500).

## References

- [1] OTSUKA K, REN X. Physical metallurgy of Ti–Ni-based shape memory alloys [J]. *Progress in Materials Science*, 2005, 50: 511–678.
- [2] MOHD JANI J, LEARY M, SUBIC A, GIBSON M A. A review of shape memory alloy research, applications and opportunities [J]. *Materials & Design*, 2014, 56: 1078–1113.
- [3] TONG Y X, SHUITCEV A V, ZHENG Y F. Recent development of TiNi-based shape memory alloys with high cycle stability and high transformation temperature [J]. *Advanced Engineering Materials*, 2020, 22: 1900496.
- [4] JIANG S Y, YU J B, ZHANG Y Q, XING X D. Mechanically-induced martensite transformation of NiTiFe shape memory alloys subjected to plane strain compression [J]. *Transactions of Nonferrous Metals Society of China*, 2020, 30: 1325–1334.
- [5] KOCKAR B, KARAMAN I, KIM J I, CHUMLYAKOV Y. A method to enhance cyclic reversibility of NiTiHf high temperature shape memory alloys [J]. *Scripta Materialia*, 2006, 54: 2203–2208.
- [6] KOCKAR B, KARAMAN I, KIM J I, CHUMLYAKOV Y I,

- SHARP J, YU C J. Thermomechanical cyclic response of an ultrafine-grained NiTi shape memory alloy [J]. Acta Materialia, 2008, 56: 3630–3646.
- [7] TONG Y X, GUO B, CHEN F, TIAN B, LI L, ZHENG Y F, PROKOFIEV E A, GUNDEROV D V, VALIEV R Z. Thermal cycling stability of ultrafine-grained TiNi shape memory alloys processed by equal channel angular pressing [J]. Scripta Materialia, 2012, 67: 1–4.
- [8] JIANG P C, ZHENG Y F, TONG Y X, CHEN F, TIAN B, LI L, GUNDEROV D V, VALIEV R Z. Transformation hysteresis and shape memory effect of an ultrafine-grained TiNiNb shape memory alloy [J]. Intermetallics, 2014, 54: 133–135.
- [9] PUSHIN V G, STOLYAROV V V, VALIEV R Z, KOUROV N I, KURANOVA N N, PROKOFIEV E A, YURCHENKO L I. Features of structure and phase transformations in shape memory TiNi-based alloys after severe plastic deformation [J]. Annales de Chimie Science des Matériaux, 2002, 27: 77–88.
- [10] PUSHIN V G, STOLYAROV V V, VALIEV R Z, LOWE T C, ZHU Y T. Nanostructured TiNi-based shape memory alloys processed by severe plastic deformation [J]. Materials Science and Engineering A, 2005, 410–411: 386–389.
- [11] PROKOSHKIN S D, KHMELEVSKAYA I Y, DOBATKIN S V, TRUBITSYNA I B, TATYANIN E V, STOLYAROV V V, PROKOFIEV E A. Alloy composition, deformation temperature, pressure and post-deformation annealing effects in severely deformed Ti–Ni based shape memory alloys [J]. Acta Materialia, 2005, 53: 2703–2714.
- [12] ZHANG X N, XIA B Y, SONG J, CHEN B, TIAN X L, HAO Y M, XIE C Y. Effects of equal channel angular extrusion and aging treatment on *R* phase transformation behaviors and  $Ti_3Ni_4$  precipitates of Ni-rich TiNi alloys [J]. Journal of Alloys and Compounds, 2011, 509: 6296–6301.
- [13] PROKOFIEV E A, BUROW J A, PAYTON E J, ZARNETTA R, FRENZEL J, GUNDEROV D V, VALIEV R Z, EGGELER G. Suppression of  $Ni_4Ti_3$  precipitation by grain size refinement in Ni-rich NiTi shape memory alloys [J]. Advanced Engineering Materials, 2010, 12: 747–753.
- [14] ZHANG D T, GUO B, TONG Y X, TIAN B, LI L, ZHENG Y F, GUNDEROV D V, VALIEV R Z. Effect of annealing temperature on martensitic transformation of  $Ti_{49.2}Ni_{50.8}$  alloy processed by equal channel angular pressing [J]. Transactions of Nonferrous Metals Society of China, 2016, 26: 448–455.
- [15] FAN Z G, XIE C Y. Phase transformation behaviors of Ti–50.9at.%Ni alloy after equal channel angular extrusion [J]. Materials Letters, 2008, 62: 800–803.
- [16] KARAMAN I, KULKARNI A V, LUO Z P. Transformation behaviour and unusual twinning in a NiTi shape memory alloy ausformed using equal channel angular extrusion [J]. Philosophical Magazine, 2005, 85: 1729–1745.
- [17] SONG J, WANG L M, ZHANG X N, SUN X G, JIANG H, FAN Z G, XIE C Y, WU M H. Effects of second phases on mechanical properties and martensitic transformations of ECAPed TiNi and Ti–Mo based shape memory alloys [J]. Transactions of Nonferrous Metals Society of China, 2012, 22: 1839–1848.
- [18] TONG Y X, HU K P, CHEN F, TIAN B, LI L, ZHENG Y F. Multiple-stage transformation behavior of  $Ti_{49.2}Ni_{50.8}$  alloy with different initial microstructure processed by equal channel angular pressing [J]. Intermetallics, 2017, 85: 163–169.
- [19] GEORGE VANDER V. Introduction to quantitative metallography [M]. Lake Bluff: Buehler Ltd, 1997: 1–5.
- [20] VASILEV L S, LOMAEV I L, ELSUKOV E P. On the analysis of the mechanisms of the strain-induced dissolution of phases in metals [J]. Physics of Metals and Metallography, 2006, 102: 186–197.
- [21] MEYERS M A, CHAWLA K K. Mechanical behavior of materials [M]. Cambridge: Cambridge University Press, 2009: 558–591.

## $Ti_{49.2}Ni_{50.8}$ 合金在等径角挤压过程中 $Ti_3Ni_4$ 析出相的演化规律

任佳瑞<sup>1</sup>, Alexander V. SHUITCEV<sup>1</sup>, 孙斌<sup>2</sup>, 陈枫<sup>1</sup>, 李莉<sup>1</sup>, 佟运祥<sup>1</sup>

1. 哈尔滨工程大学 材料科学与化学工程学院 材料加工及智能制造研究所, 哈尔滨 150001;

2. 哈尔滨工程大学 材料科学与化学工程学院 分析测试中心, 哈尔滨 150001

**摘要:** 采用透射电子显微镜研究  $Ti_{49.2}Ni_{50.8}$  合金中  $Ti_3Ni_4$  析出相在等径角挤压及中间退火过程中的演化规律。固溶态  $Ti_{49.2}Ni_{50.8}$  合金在 450 °C 时效处理 10~60 min 以获得尺寸为 37~75 nm 的  $Ti_3Ni_4$  析出相。在 450 °C 等径角挤压处理 1 道次后, 时效处理 10 min 和 30 min 试样中  $Ti_3Ni_4$  析出相完全溶解; 而在时效处理 60 min 试样中  $Ti_3Ni_4$  析出相尺寸减小。 $Ti_3Ni_4$  析出相完全溶解的临界尺寸范围为 37~68 nm。等径角挤压态试样的位错密度取决于  $Ti_3Ni_4$  析出相的初始尺寸。随初始时效时间从 10 min 延长至 60 min, 试样的位错密度先增加然后降低。

**关键词:** TiNi 形状记忆合金; 等径角挤压; 位错; 析出;  $Ti_3Ni_4$  相

(Edited by Wei-ping CHEN)